

Behavior of overlapping Cold Formed Z-Beams

Sally Hosny Taha, Dr.Rimon Aziz Samaan, Prof.Dr.Nahla K. Hassan

Abstract— Z-section is one of the most common cold-formed purlins. Its lapping ability provides continuity, and double thickness at the support regions. Four different types of systems may be found in modern roofs; single span, double span, multi-span with sleeves and multi-span with overlaps is the most popular. Four verification cases: simple and overhanging beams are conducted, using FEM to investigate the structural behaviour of lapped connections over the internal supports in multi-span systems with overlap. Results are compared with code and previous experimental work and good agreement is achieved.

In this study, The moment resistance of overhanging Z-purlin with constant thickness (1.5 mm) ,different heights (142,172,202 and 232 mm) and overlap lengths (0.1L to 0.5L) ,where L is the back span length are investigated under combined bending and shear using ANSYS14.00. For each lap length and height, models were also conducted with and without straps with either restrained compression flanges or not.

Index Terms— Cold Formed ,overhanging beams ,Z-beams ,Finite Element.

I. INTRODUCTION

Cold-formed steel sections are lightweight building materials with high strength to self-weight ratios. They are suitable for building construction owing to their versatility in applications, and ease of fabrication and installation. In general, both cold-formed steel C sections [1-3] and Z sections [4-8] are widely used in building construction. The section depths typically range from 100 to 350 mm while the section thicknesses typically range from 1.2 to 3.0 mm [9-11]. Z-sections are recommended for the use as purlins for a variety of reasons, the main one is that their principal axis often coincides with the roof pitch thus enabling the designer to take full advantage of the strength of this section. The second advantage is that they offer easier fixing, since the top flange does not interfere with the fixing equipment. The purlins are connected to the rafter using angles which provide some torsional restraint to the section otherwise it may twist. The third one is that, Z section is better than C section because it can easily lap the Z section at support with the Z section face to face but in case lapping the C section they will be back to back. This requires the seam lines of the roof metal deck to be shifted between panel which is impossible to achieve [12].

Four different types of purlin systems may be found in modern roofs with different degrees of continuity: (i) single span, (ii) double span, (iii) multi-span with sleeves, and (iv) multi-span with overlaps [6]. The load carrying capacities of these purlin systems depend on many factors, such as steel

grades, section shapes and sizes of purlin members, restraints provided by attached roof cladding and intermediate bracing members, and connection configurations at purlin–rafter supports. In practice, multi-span purlin systems with overlaps are the most popular owing to their high structural efficiency and simple installation of purlin–rafter connections. The general member arrangement of multi-span purlin systems with overlaps can be easily modeled by two cases as a simple beam [5-7] or as an overhanging beam [8].

The main objectives of this paper is to develop Finite element models using Ansys14 [13] to simulate the experimental behavior of lapped connections between cold-formed steel Z sections by verifying the results obtained by the proposed finite element model against experimental investigation performed by others [5, 7, 8]. A comprehensive set of previous experimental work is provided to illustrate the various capabilities of the nonlinear finite element proposed model. These cases are selected to cover a wide range of applications both in geometry and loading of the tested specimens.

In the parametric study, The moment resistance of overhanging Z-purlin with constant thickness (1.5 mm) ,different heights (142,172,202 and 232 mm) and overlap lengths (0.1L to 0.5L ,where L is the back span length) are investigated under combined bending and shear using ANSYS14.00 [13]. For each lap length and height, models were also conducted with and without straps with either restrained compression flanges or not.

II. VERIFICATION OF EXPERIMENTAL AND FINITE ELEMENT MODEL

The verification cases consists of two parts; experimental work and codes. Three main different experimental studies that were conducted by three different researchers; Cao Hung Pham 2014 [5], Ahmad A. Ghosn 1995 [7], Ain Shams and Zamil 2014 [8] were verified to evaluate the performance of the FE model for different specimens. The second part, proposed models were compared with the flexural strength code equations of AISI 2007 [14] for beams subjected to combined bending and shear. The accurate results of FE analysis can be utilized to predict the ultimate loads of cold-formed lapped Z-section purlin subjected to combined bending and shear.

A. F.E. Model Geometry

A detailed finite element model was developed to predict maximum load and failure modes of multi span Z-purlins. The Z-purlins (Fig 1), Channels and straps (Fig 2) were modeled in ANSYS using four node shell element (SHELL181) but the test rig (Fig 3) and bearing plates (Fig 4) were generated using 3D-deformable solid elements (SOLID185). The head and nut of bolts together with the shank part of bolt (Fig 5) were also modeled using (SOLID185). All elements were assigned as normal steel properties. CONTACT178 is used to connect the nodes of

Manuscript received November 11, 2014.

Sally Hosny Taha, Steel Structural department, Suez Canal university/ Faculty of Engineering/ Ismailia, Egypt, +201221583048.

Dr.Rimon Aziz Samaan, Steel Structural department, Ain Shams university / Faculty of Engineering / Cairo, Egypt, +201001419553.

Prof.Dr.Nahla K. Hassan, Steel Structural department, Ain Shams university / Faculty of Engineering / Cairo, Egypt, +201222373098.

i)the two overlapped Z beams as shown in Fig 6. ii)Straps and flanges of Purlins iii)channel and web of Z section. The 10 mm element mesh was selected that gave high accuracy within a reasonable time. For modeling of boundary conditions, two single points (A,B) were modeled in the center of two bearing plates of thickness 20mm (Fig 7), one hinged support and the other is roller as shown in Fig 8. Because of the symmetric cross section, a symmetry boundary condition was also applied on a plane of nodes according YZ plane for the whole model, Fig 3,8. A concentrated load was applied over a 30mm head plate Fig 3. a non-linear analysis that considered material and geometric non-linearity was performed using the arc-length method. The maximum and minimum multiplier of the reference arc-length radius was 1 and 0.0001, respectively.

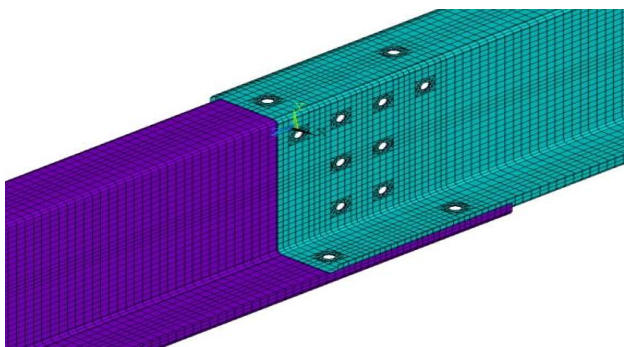


Fig 1. Shell Element of cold formed Z-section

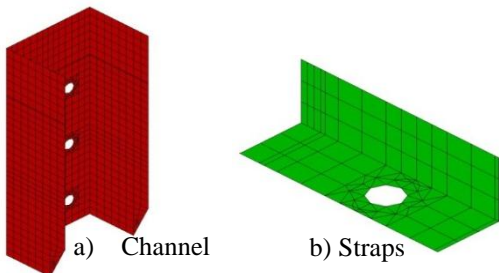


Fig 2. Shell Element of stiffeners

B. Symm. B.C.

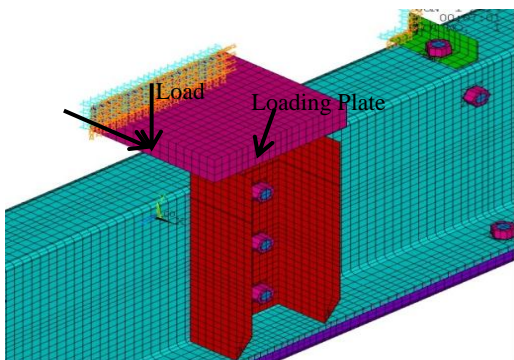


Fig 3. Loads on the Finite Element Model.

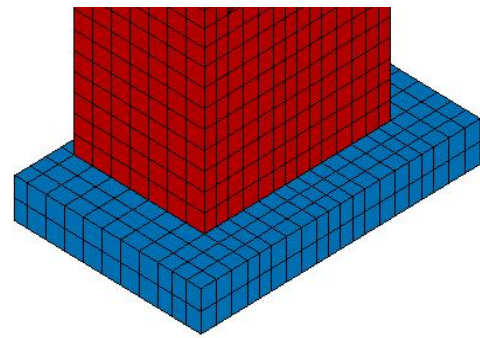


Fig 4. Solid Element of bearing plate

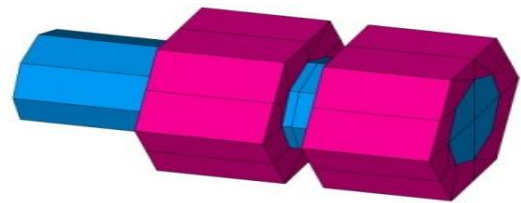


Fig 5. Solid Element of bolts

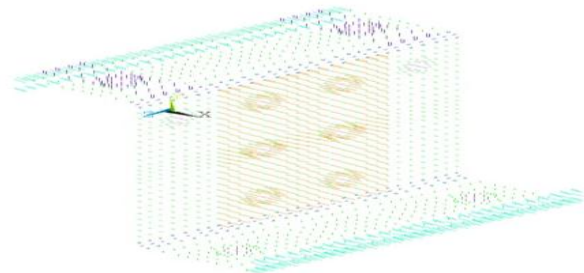


Fig 6. contact node to node

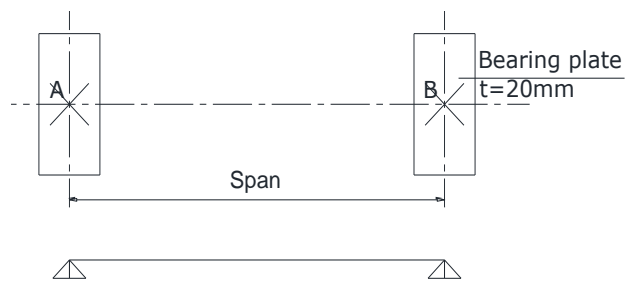


Fig 7. Plan of Bearing plate.

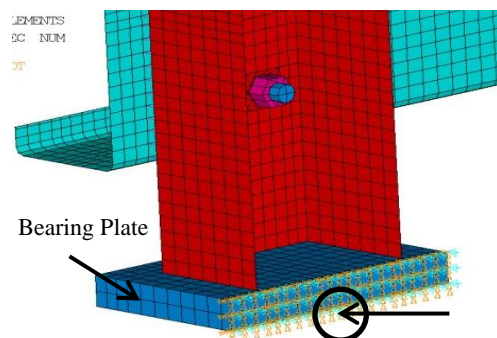


Fig 8. One hinged support on the center of bearing plate.

F.E. Validation of Experimental Results

Case I; Cao Pham (2014) [5]

When you submit your final version, after your paper has been accepted, prepare it in two-column format, including figures and tables.

The experimental program comprised a total of four tests. All tests were performed in the 2000 kN capacity for a continuous lapped Z purlin connection based on the simplified analysis as a simple beam.

The Z-section purlins were tested in pairs with top flanges facing inwards and with a gap between them to ensure that the inside assembly was possible. Two tests were conducted with six 25 × 25 × 5EA straps which were uniformly and symmetrically connected by self-tapping screws on the top flanges as shown in Fig 10. The purpose of these two straps is to prevent distortion of the top flanges under compression caused by bending moment. It is believed that sheeting screw fastened to the top flanges will have a similar effect to the straps in the tests with straps. other tests were conducted without Straps Fig 9.

using same elements as previously mentioned, the F.E. mesh and boundary conditions as shown in Fig 11. The comparison between the experimental program results and the proposed numerical model results are summarized in Table 1.

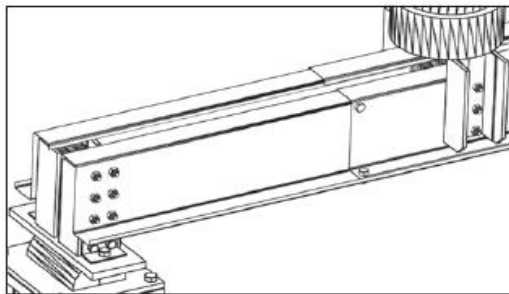


Fig 9. Test without Straps

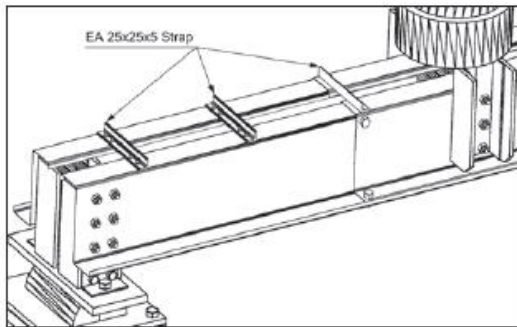


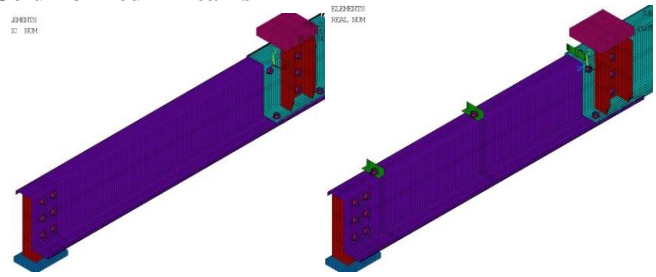
Fig 10. Test with straps

Table 1. Comparison between finite element model and experimental results

It is evident for Table 1, that the finite element model results are in good agreement with the experimental results: ratio within a maximum deviation of 8 %.

As shown in Fig 12 and Fig 13, the results of the F.E. models and the experimental work were in good agreement. The load dropped more suddenly in Specimen with straps (Fig 13) than that without the straps as shown in Fig 12 due to the local buckling mode in the flange.

Good agreement in various failure modes was achieved for



a) Without Straps b) With Straps

Fig 11. Finite Element Model.

the F.E. models with the experimental work. For beams without Straps Fig 14, the top flange of the lower Z-section buckled and was pulled in and down. Simultaneously, the top flange of the upper Z-section was twisted and lifted due to the discontinuity of the connection in bending. But with Straps

Specimen	a (m)	Experimenta	FEM	Acc (%)
		l	Model results	
		Failure load (kN)	(kN)	
MVw-Z20015	100	34.31	36.47	-6.3
MVw-Z20015	300	48.041	46.42	3.4
MVs-Z20015	100	51.89	55.5	-7.0
MVs-Z20015	300	68.00	62.4	8.2

Fig 15, local buckling occurred in the top flange of the upper Z-section. No distortion at the cross-section was observed

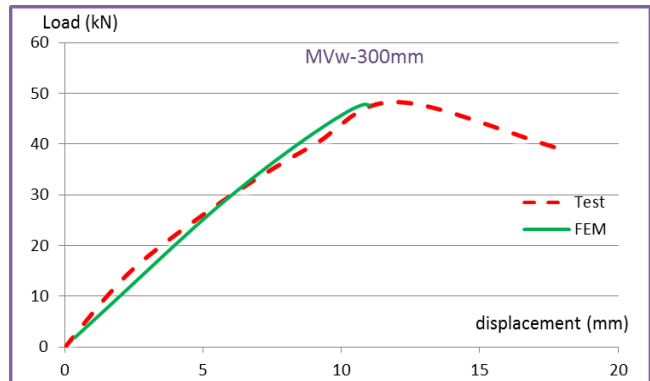


Fig 12. Load and vertical displacement relations of MVw-Z20015-300 mm

due to the straps which may significantly increase the

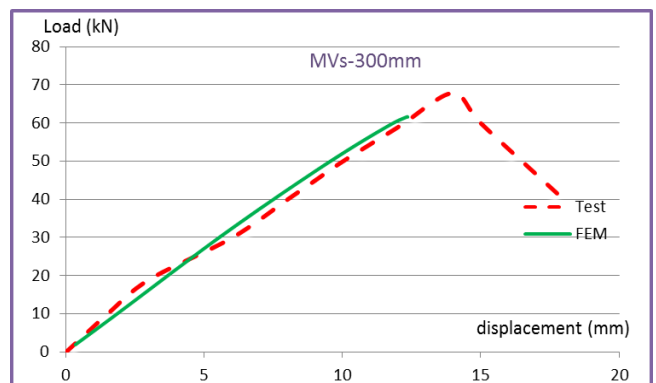


Fig 13. Load and vertical displacement relations of MVs-Z20015-300 mm

capacity and enhance the continuity of the lapped connection.

consideration initial imperfection as shown in Table 2

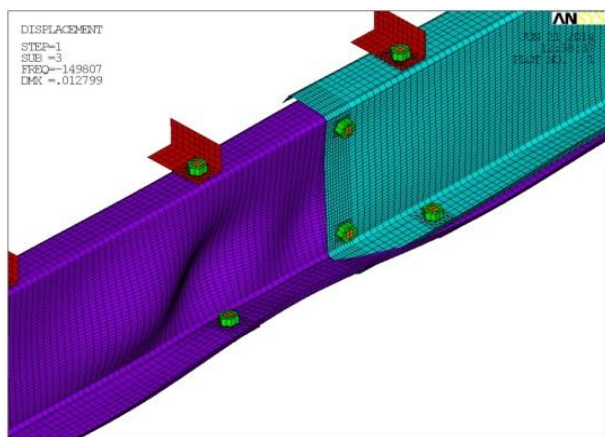


Fig 17.Eigenmode 3 of FEM of Z-section

Table2. Comparison between Finite Element model and Experimental analysis

Sec	Lap cm	Experi-mental model	FE without imperfe-c-tion	acc. %	FE with imperfe-ction	acc. %
		Failure load (kN)	Failure load (kN)		Failure load (kN)	
Z9.5 x07 5	0	26.6	34.0437	27.98	30.88	16.09
	121.92	53.38	58.41	6.07	49.73	-9.7
		47.59				
		55.07				
		55.07				
	152.4	55.56	67	19.3	64.9	15.5
60.69	69.39	61.98	-10.7	67.61	-2.6	
121.92	84.07	107.4	27.75	103.9	23.6	
Z8.0 x06 0	0	17.79	20.46	15	20.1	13
	60.69	25.58	25.7	0.47	24.74	-3.3
	121.92	31.71	37.3	17.63	34.14	7.66
Z8.0 x07 5	0	23.49	26.14	11.28	22.66	-3.5
	60.69	32.25	31.38	-2.7	29.9	-7.3
	121.92	47.95	45.87	-4.34	43.33	-9.6
Z8.0 x09 9	0	39.59	42.81	8.13	37.44	-5.4
	60.69	46.48	53.37	14.82	48.04	3.36
	121.92	66.85	78.39	17.26	72.78	8.87

The third verification case was an experimental program between Faculty of Engineering, Ain Shams university and Zamil Steel company, Structural Department. The program was conducted to study Zee sections continuity provided by overlapping an overhanging Z-purlins with 1.5m back span and 1.5m cantilever length was conducted. Over the internal support, the two overlapped Z-beams was bolted together through web only as shown in Fig by M12 high tensile bolts. The model was laterally supported with upper straps only represented the corrugated sheets. The loading setup at the end of cantilever is shown in Fig 20.

For the internal support, The overlapped beams were connected to the support by two bolts; one of them connected the overlapped Z-beams and upper bearing flange. The other connected only the overhanging beam and the upper flange of the support, Fig 19.



Fig19.Internal Support.

As for the external support, end beam was bolted to built-up frame through 90x90x9 cleat angle and no bolts are used in the lower flange.

The results of both experimental and analytical analyses were compared to each other. While the failure load for experimental model was 1.6 ton, the finite element model was 1.668 ton that shows good agreement between the finite element model and the experimental results.

The failure modes of both the finite element model and experimental specimen were compared and good agreement was achieved as shown in Fig 21. Flange distortional buckling was severe due to the compression stress caused at the bottom flange by the bending moment. Local buckling occurred in the web under the combined bending and shear

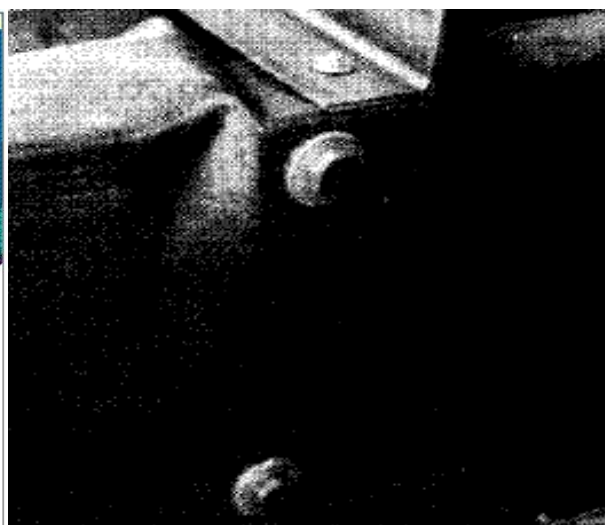
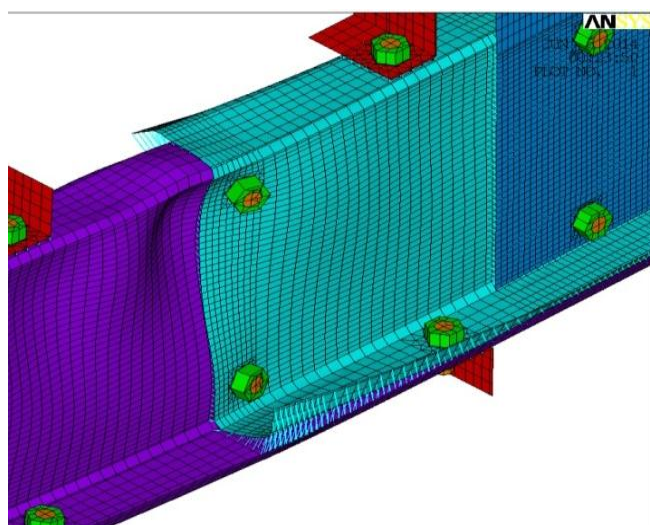


Fig 18. Typical Failure Pattern of Tested Beams and Finite Element Models

stresses.

Case III; Ain Shams and Zamil Steel Experimental Program

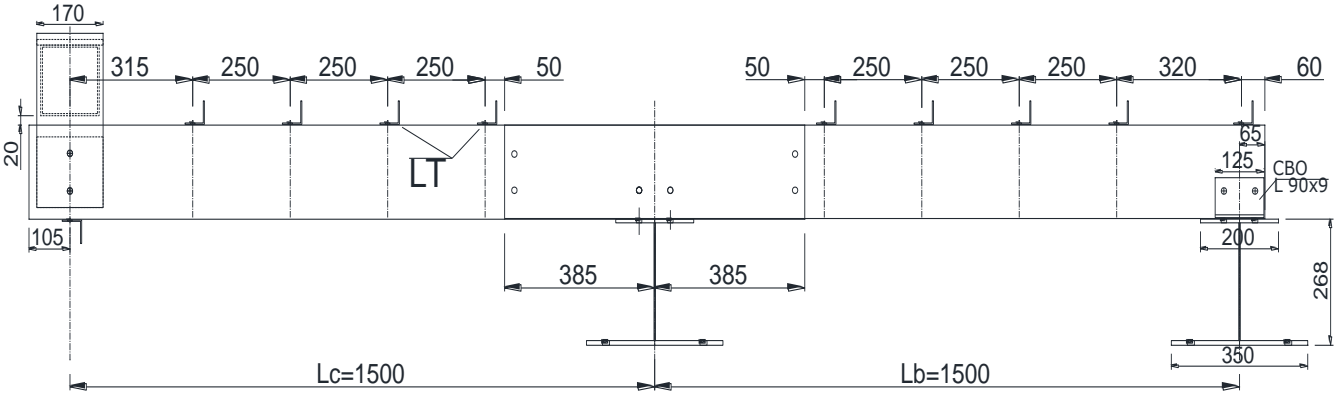


Fig 20. Model geometry

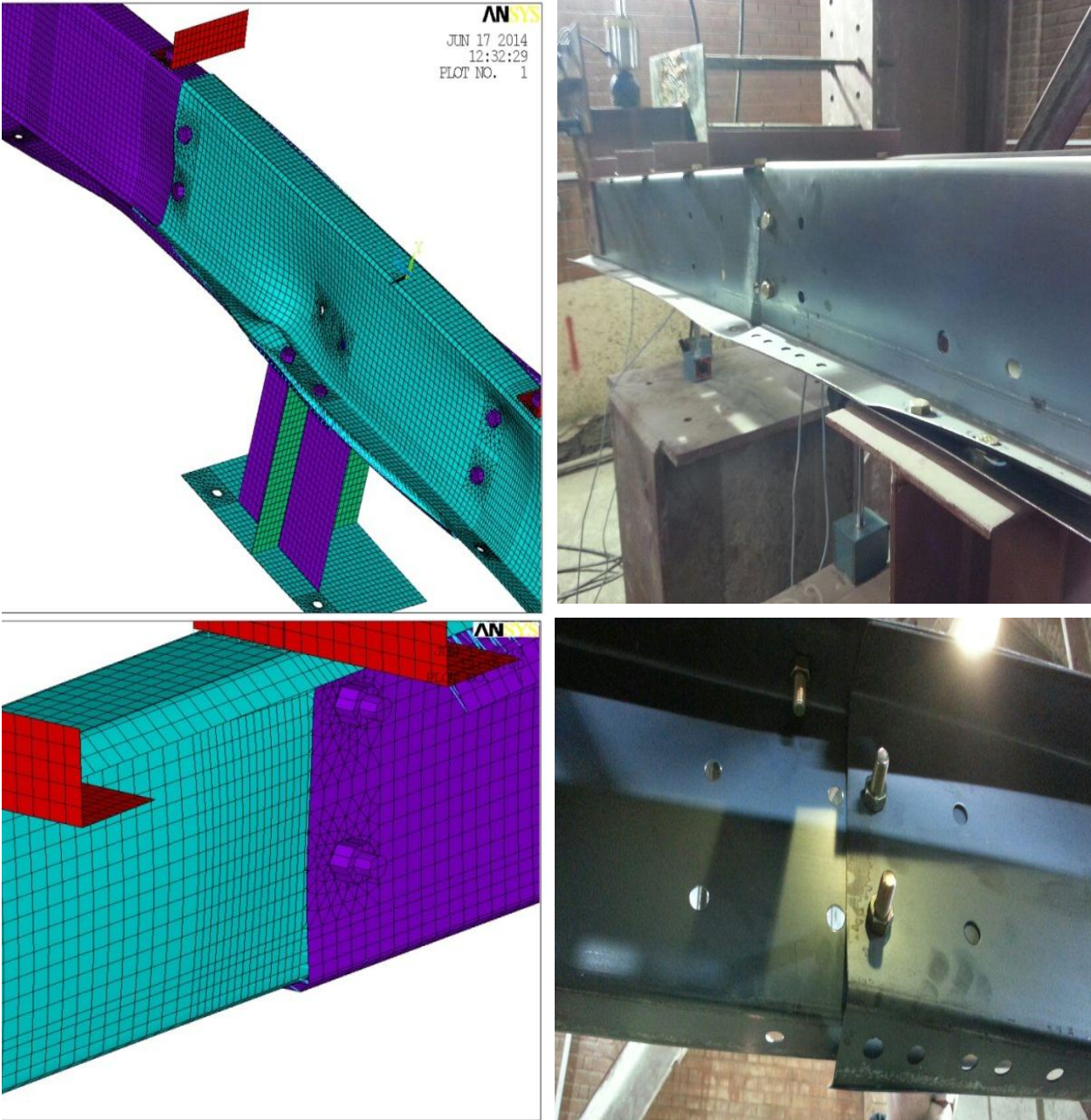


Fig 21. FE and Experimental modes of Failure

FE validation of AISI Code.

The required flexural strength, M, and required shear strength, V, shall also satisfy the following interaction equation which is determined from Section C3.3 at AISI2007:

$$\sqrt{\left(\frac{\Omega_b M}{M_{nco}}\right)^2 + \left(\frac{\Omega_v V}{V_n}\right)^2} \leq 1.0 \dots \dots \dots (Eq. C3.3.1)$$

- 1) AISI2007

The model consist of an overhanging beam as shown in Fig 23 with 1.5m back span and 1.5 cantilever length under concentrated load at the end of cantilever. The Load was applied through the web using box loading and stiffener web plate. Fig 22 and Table 3 show the Z-section dimension and properties.

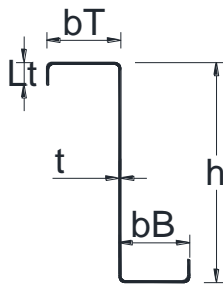


Fig22.Z-section properties

Table 3.Z-section Dimensions.

Section	Thic kness (t) mm	Depth (h) mm	Top flange (bT) mm	Bottom flange (bB) mm	Lip length (Lt) mm
142Z15	1.5	142	60	55	20
142Z16	1.6	142	60	55	20
142Z18	1.8	142	60	55	20
172Z15	1.5	172	65	60	20
172Z16	1.6	172	65	60	20
202Z18	1.8	172	65	60	20
202Z15	1.5	202	65	60	20
202Z16	1.6	202	65	60	20
202Z18	1.8	202	65	60	20
232Z15	1.5	232	76	69	20
232Z16	1.6	232	76	69	20
232Z18	1.8	232	76	69	20

The sections were tested in pairs under different cases of laterally braced by 50x50x3 steel angles. These cases were; i)with both top and bottom flanges, ii)with upper straps only iii)without straps. For all steel elements, yield stress fy used was taken 345 MPa. Young's modulus of elasticity was 210,000 MPa. Poisson Ratio is 0.3 and tangent Modulus is taken 1000 MPa.

Same boundary condition and elements were used as the pervious verification models. The ANSYS results were generally in good agreement with Code values for the ultimate loads and modes of failure as shown in Table 4 and Fig 24. All results in Table 4 are for only single Z-purlin.

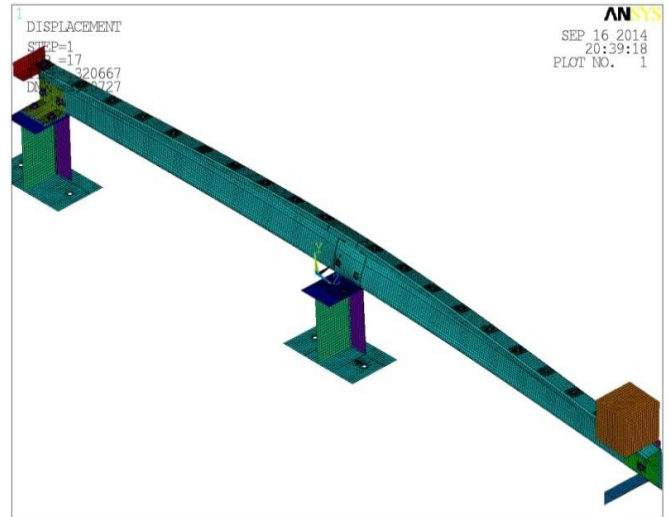


Fig 24.Failure Mode of Z172WL16

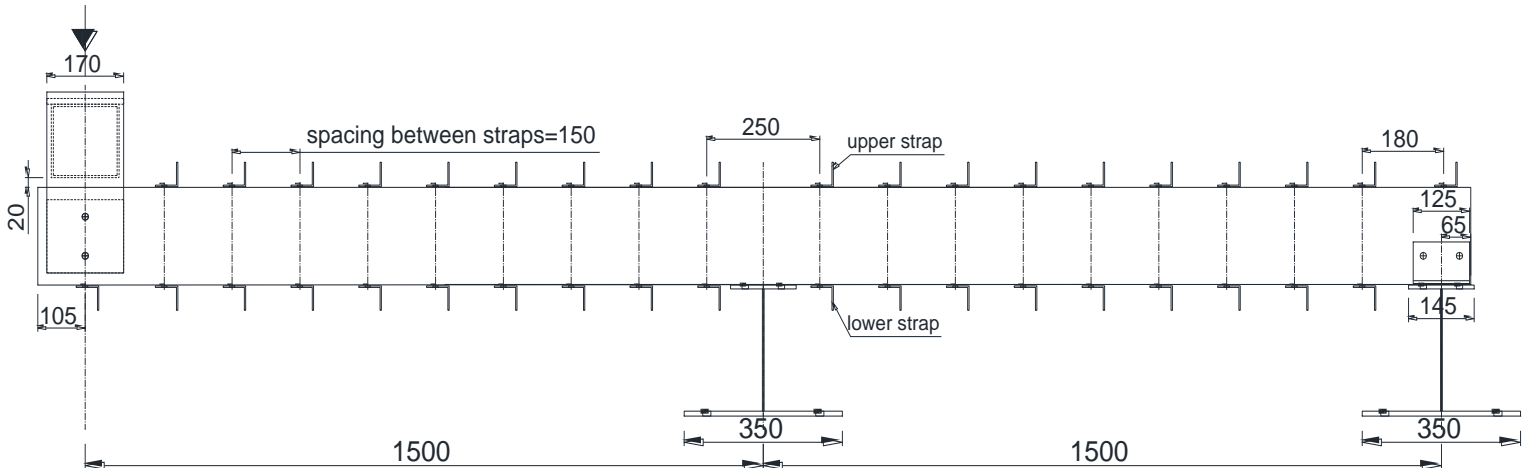


Fig 23.Model geometry

Table 4. AISI and FE models Results

Model		Lx (m)	Ly (m)	Lt (m)	AISIP (t)	Failure Mode	F.E. P (t)	acc.%
142Z15	Z142UPDNL15	0.18	0.25	0.25	0.385	Y	0.390	-1%
	Z142UPonLy15	1.5	1.5	1.5	0.383	L.T.B	0.390	-2%
	Z142WL15	1.5	2.1	1.5	0.352	L.T.B	0.356	-1%
172Z15	Z172UPDNL15	0.18	0.25	0.25	0.496	D.B	0.472	5%
	Z172UPonLy15	1.5	1.5	1.5	0.496	D.B	0.474	4%
	Z172WL15	1.5	2.1	1.5	0.469	L.T.B	0.436	5%
202Z15	Z202UPDNL15	0.18	0.25	0.25	0.577	D.B	0.542	6%
	Z202UPonLy15	1.5	1.5	1.5	0.577	D.B	0.542	6%
	Z202WL	1.5	2.1	1.5	0.563	L.T.B	0.504	5%
232Z15	Z232UPDNL15	0.18	0.25	0.25	0.663	D.B	0.621	6%
	Z232UPonLy15	1.5	2.8	1.5	0.629	L.T.B	0.607	3%
	Z232WL15	1.5	3	1.5	0.606	L.T.B	0.578	5%
142Z16	Z142UPDNL16	0.18	0.25	0.25	0.419	Y	0.424	-1%
	Z142UPonLy16	1.5	1.5	1.5	0.416	L.T.B	0.429	-3%
	Z142WL16	1.5	2.1	1.5	0.382	L.T.B	0.387	-1%
172Z16	Z172UPDNL16	0.18	0.25	0.25	0.543	D.B	0.522	4%
	Z172UPonLy16	1.5	1.5	1.5	0.543	D.B	0.528	3%
	Z172WL16	1.5	2.1	1.5	0.498	L.T.B	0.481	3%
202Z16	Z202UPDNL16	0.18	0.25	0.25	0.636	D.B	0.603	5%
	Z202UPonLy16	1.5	1.5	1.5	0.636	D.B	0.603	5%
	Z202WL16	1.5	2.1	1.5	0.576	L.T.B	0.555	4%
232Z16	Z232UPDNL16	0.18	0.25	0.25	0.738	D.B	0.689	7%
	Z232UPonLy16	1.5	2.8	1.5	0.691	L.T.B	0.684	1%
	Z232WL16	1.5	3	1.5	0.664	L.T.B	0.641	3%
142Z18	Z142UPDNL18	0.18	0.25	0.25	0.492	Y	0.503	-2%
	Z142UPonLy18	1.5	1.5	1.5	0.489	L.T.B	0.510	-4%
	Z142WL18	1.5	2.1	1.5	0.449	L.T.B	0.449	0%
172Z18	Z172UPDNL18	0.18	0.25	0.25	0.634	Y	0.628	1%
	Z172UPonLy18	1.5	1.5	1.5	0.634	Y	0.633	0%
	Z172WL18	1.5	2.1	1.5	0.579	L.T.B	0.572	1%
202Z18	Z202UPDNL18	0.18	0.25	0.25	0.755	D.B	0.726	4%
	Z202UPonLy18	1.5	1.5	1.5	0.755	D.B	0.726	4%
	Z202WL18	1.5	2.1	1.5	0.673	L.T.B	0.663	1%
232Z18	Z232UPDNL18	0.18	0.25	0.25	0.890	D.B	0.838	6%
	Z232UPonLy18	1.5	2.8	1.5	0.811	L.T.B	0.831	-2%
	Z232WL18	1.5	3	1.5	0.778	L.T.B	0.697	10%

Where;

- Lx: Unbraced length of member for bending about x-axis,
- Ly : Unbraced length of member for bending about y-axis,
- Lt : Unbraced length of member for twisting ,
- P: Required strength for concentrated load or reaction in the presence of bending Moment,
- L.T.B: Lateral torsional buckling mode,
- D.B: Distortional Buckling failure mode,
- Y:Initiation of yielding Mode

III. PARAMETRIC STUDY

The moment resistance of overhanging and overlapping Z-purlins with different heights and overlap lengths (Llap) are investigated under combined bending and shear. The multi-span purlin systems with overlaps are simplified by overhanging beam, Fig 25. The back span (L) of Z-purlin is taken 1.5 m and 1.5 m overhanging length (Lc). For each lap length and different heights, models were also conducted and studied with and without straps with either restrained compression flange or not as shown in Fig 27.

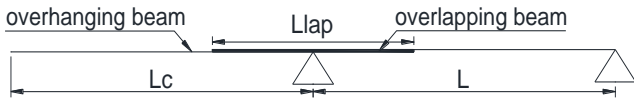


Fig 25. overlapped overhanging beam.

Dimension of Z-section

The Z-sections feature one broad and one narrow flange, sized so that two sections of the same size can fit together snugly, making them suitable for lapping. Z-dimensions (Fig 26) are given in Table 5. The purlins were modeled in pairs as shown in Fig to avoid torsional and lateral buckling effects caused by the shear flow with top flanges facing inwards and with a constant gap between 300mm to ensure that the inside assembly was possible.

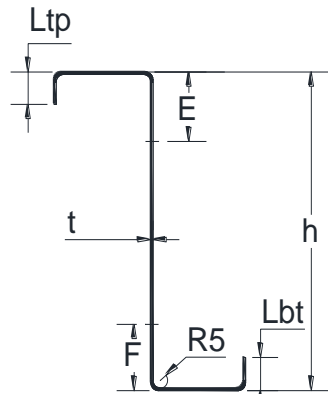


Fig 26. Geometry of Z-section.

For all steel elements, yield stress fy used was 345MPa. Young's modulus of elasticity was 210,000 MPa. Poisson Ratio is 0.3.

Sec	t mm	h mm	Top bf mm	Bott-om bf mm	Ltp mm	Lbt mm	E m	F mm
142 Z 15	1.5	142	60	55	19	21	44	42
172 Z 15	1.5	172	65	60	19	21	44	42
202 Z 15	1.5	202	65	60	19	21	44	42
232 Z 15	1.5	232	76	69	19	21	44	42

Table 5.Dimension of Z-section

previous studies [5-7], the lapping process enhanced the load capacity of beams with lap length to span ratios (Llap/L) from (0.1L to 0.5L).

All steel elements were connected using φ12 high tensile bolts grade M8.8 with horizontal edge distance 25mm. The lapped configuration is detailed in Fig 28 and Fig29.

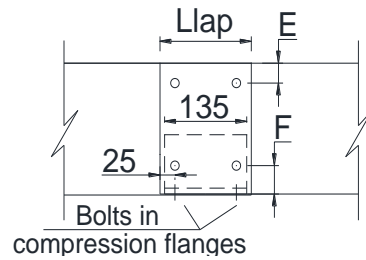


Fig 28. Bolt configuration at lap length 0.1L.

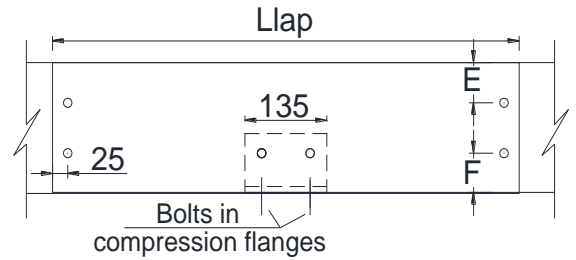


Fig29. Bolt configuration at lap length from (0.2L to 0.5L).

In the parametric study, The models were conducted with and without mid angles that connected to top bearing flange with or without restraining compression flanges. 50 × 50 × 3 straps which were uniformly and symmetrically connected as shown in Fig 27. Spacing between them was 150 mm (0.1L). The Study Models were conducted at three cases; i)without Straps ii)upper straps only iii)both upper and lowers straps.

At the end of cantilever, the concentrated load was applied on box loading with 150 mm height and 3 mm thickness to ensure that the load is applied uniformly. The load then was transferred to the web through load plate of 170 mm width and 8 mm thickness which were connected to the purlin web and stiffener web plate of 170 mm width and 5 mm thickness by two bolts as shown in Fig 30.

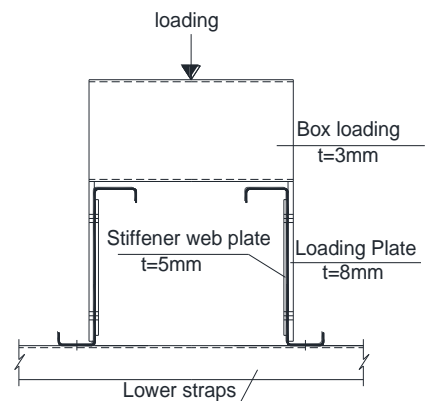


Fig 30.Loading part.

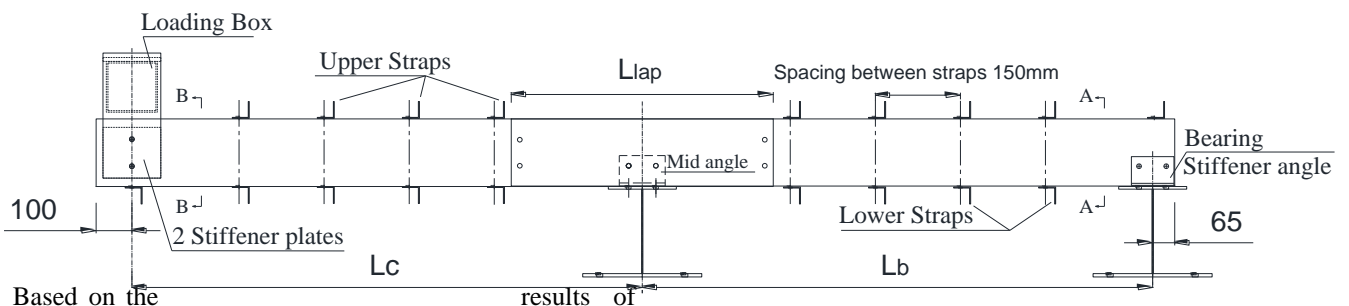


Fig 27.Schematic drawing of parametric study model.

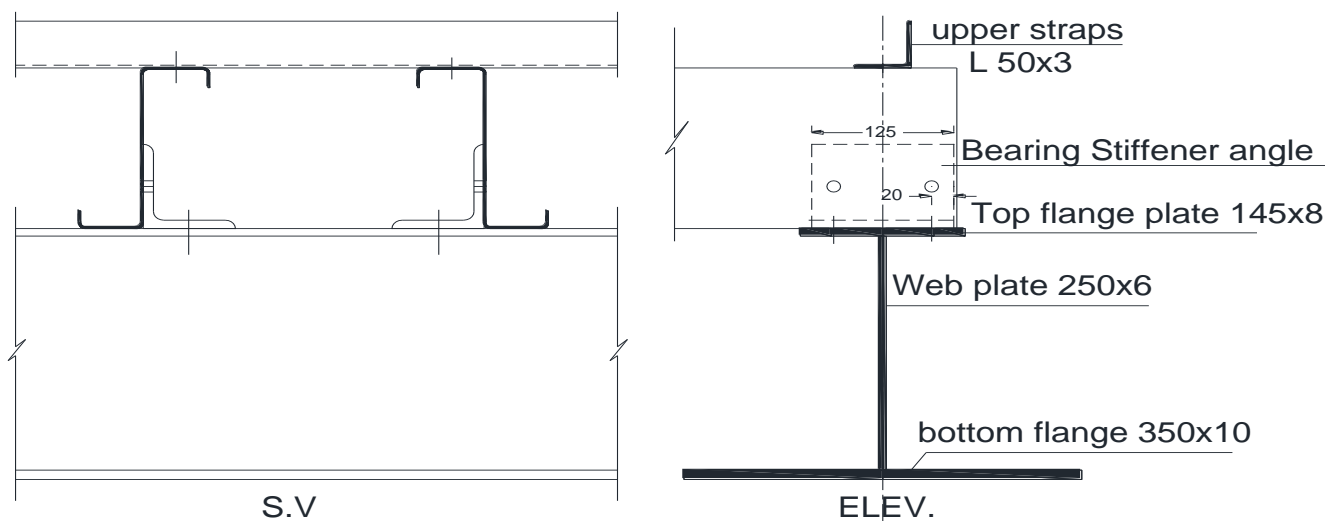


Fig 31. End bearing.

These beams were rested on two built-up frames as in Fig 31 top flange plate 145 mm x 8 mm, bottom flange plate 350 mm x 10 mm and web plate 250 mm x 6 mm.

A Non-linear finite element analysis was executed and both geometrical and material nonlinearities were considered using same element and boundary conditions as in the verification cases, Fig 32.

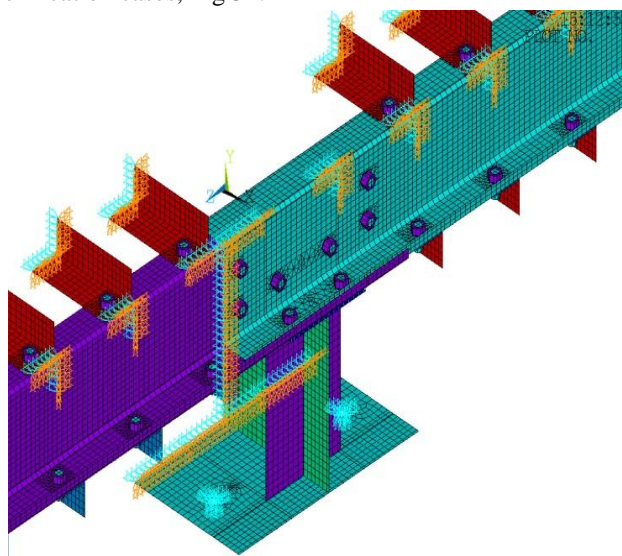


Fig 32. Finite Element model

IV. RESULT DISCUSSION

All results of these beams are for single Z

A. Effect of Presence of mid angle in case of restrained compression flanges

Table 6 shows the relationship between the ultimate moment capacity and the lap length in case of both straps. In Figs (33,34,35) in case of i)both straps ii)upper straps only iii)without straps, the effect of mid angle on the ultimate moment capacity of the section for lap length (0.2L to 0.5L) is less than 5%, while for lap length less than 0.2L it increases proportionally with height of Z from (2.5~20%). The usage of mid angle has a significant effect at lap length 0.1L because of the high stress concentration that develop at small overlap length as in Fig 36 and Fig 37 therefore the use of any stiffeners will be effective.

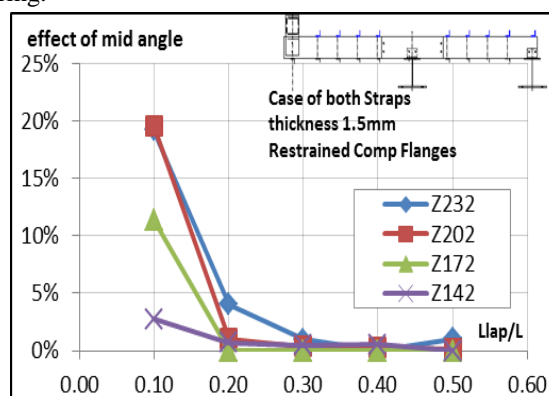


Fig 33. effect of mid angle under different overlaps in case of both straps.

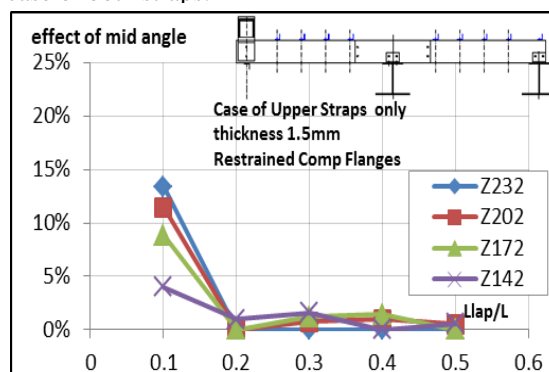


Fig 34. effect of mid angle under different overlaps in case of upper straps.

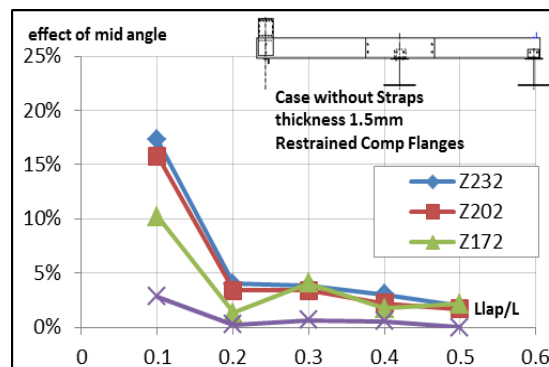


Fig 35. effect of mid angle under different overlaps in case without straps.

Behavior of overlapping Cold Formed Z-Beams

Table 6. Results of different lap lengths in case of both straps.

Model	Llap	Lap length mm	with mid angle	without mid angle
			Moment capacity (m.t)	Moment capacity (m.t)
Z232	0.1L	150	1.28	1.08
	0.2L	300	1.40	1.35
	0.3L	450	1.51	1.49
	0.4L	600	1.62	1.63
	0.5L	750	1.74	1.72
Z202	0.1L	150	1.05	0.88
	0.2L	300	1.15	1.14
	0.3L	450	1.25	1.24
	0.4L	600	1.35	1.34
	0.5L	750	1.46	1.45
Z172	0.1L	150	0.84	0.75
	0.2L	300	0.96	0.96
	0.3L	450	1.04	1.04
	0.4L	600	1.14	1.13
	0.5L	750	1.23	1.23
Z142	0.1L	150	0.61	0.60
	0.2L	300	0.74	0.73
	0.3L	450	0.81	0.81
	0.4L	600	0.88	0.88
	0.5L	750	0.95	0.95

B. Effect of restraining compression flanges in presence of mid angle

The effect of restraining compression flanges using two bolts is directly proportional to the height as in figures 38-40. i) in case of both straps (Table 7), it slightly affect the maximum moment within 0~7% for lap length ranging from (0.2L to 0.5L) and this effect increases for lap length less than 0.2L up to 20% . ii) in both cases of using upper straps or without straps, restraining compression flanges has a significant effect especially on lap length less than 0.2L up to 40% and from(5~25)% for lap length ranging from (0.2L to 0.5L). The effect of restraining compression is also inversely proportional to the overlap length. But this inversed in case of i) upper straps only, from lap length 0.4L (Fig 38). ii) in case without straps, from lap length 0.3L (Fig 39). It can be concluded that restraining the compression flanges is more effective in case of upper straps only or without straps as the failure modes in these cases is due to distortional buckling in bottom flanges as shown in Fig 41-43 so using bolts at compression flanges restrained them as shown in Fig 44-46.

Table 7. Results of different lap lengths with both straps

Model	Lap length (mm)	Restrained comp. flanges	unrestrained comp flanges
		Moment capacity (m.t)	Moment capacity (m.t)
Z232	150	1.28	1.01
	300	1.40	1.31
	450	1.51	1.46
	600	1.62	1.59
	750	1.74	1.72
Z202	150	1.05	0.86
	300	1.15	1.10
	450	1.25	1.22
	600	1.35	1.34
	750	1.46	1.45
Z172	150	0.84	0.72
	300	0.96	0.92
	450	1.04	1.02
	600	1.14	1.12
	750	1.23	1.21
Z142	150	0.61	0.57
	300	0.74	0.71
	450	0.81	0.79
	600	0.88	0.87
	750	0.95	0.94

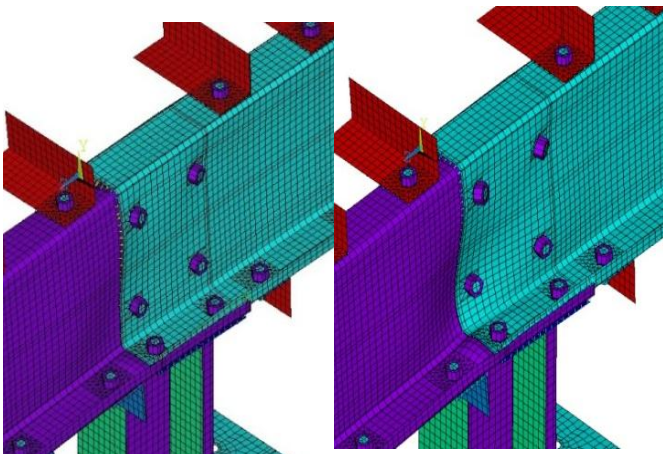


Fig 36. Failure mode of 0.1L with and without mid angle.

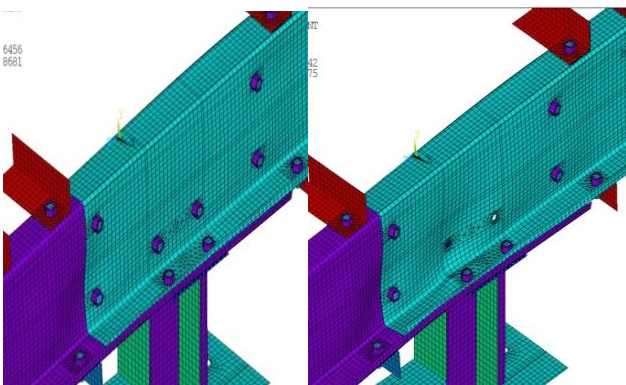


Fig 37. Failure mode of from (0.2L to 0.5L) with and without mid angle.

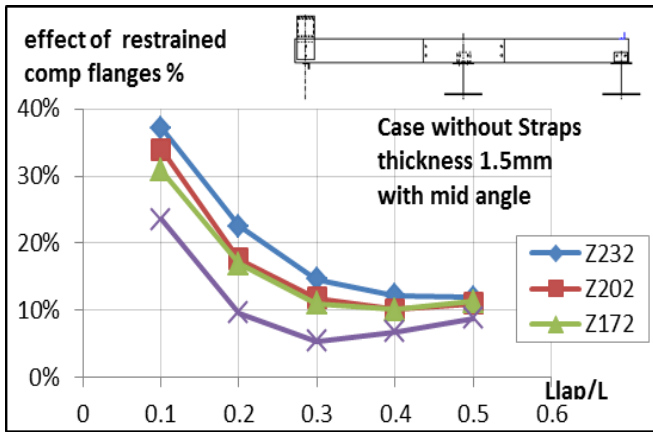


Fig 40. Results of different lap length in case without straps.

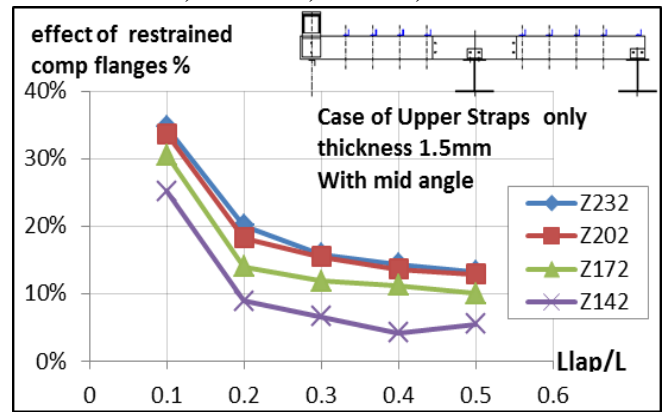


Fig 39. Results of different lap length in case of upper straps only.

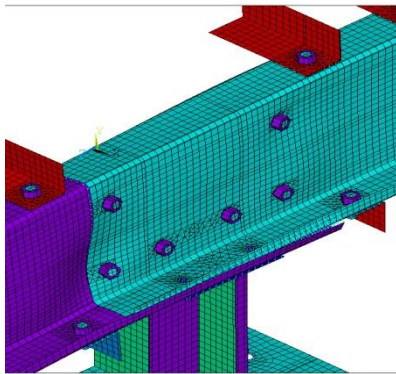


Fig 41. Failure mode in case of both straps without restraining compression flanges

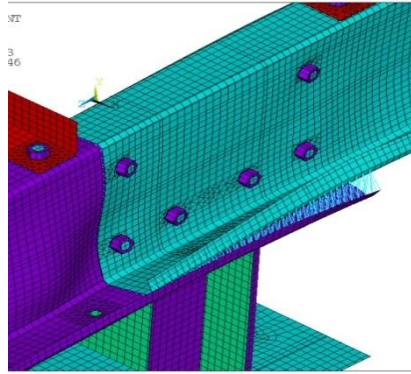


Fig 42. Failure mode in case of upper straps without restraining compression flanges

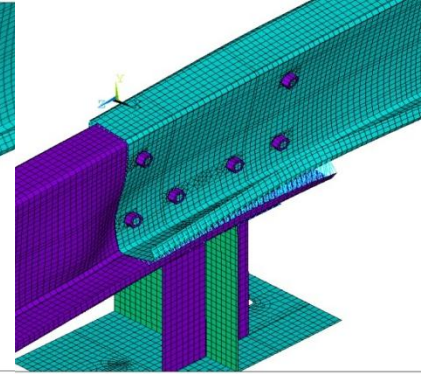


Fig 43. Failure mode in case of both straps without restraining compression flanges

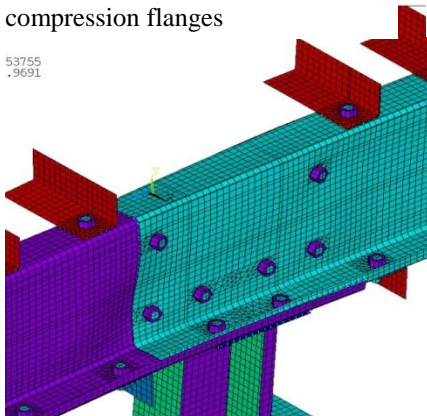


Fig 44. Failure mode in case of both straps with restraining compression flanges.

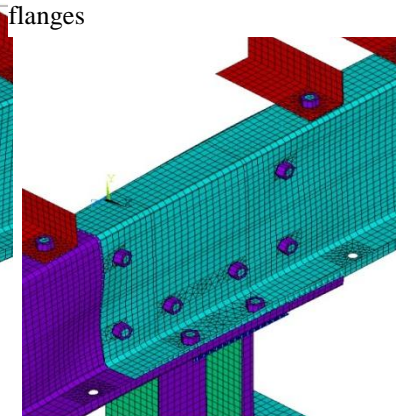


Fig 45. Failure mode in case of both straps with restraining compression flanges

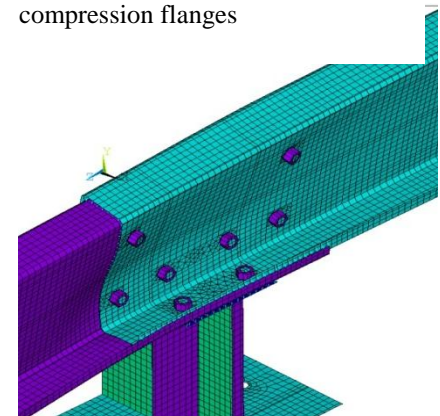


Fig 46. Failure mode in case of both straps with restraining compression flanges

C. Comparison between restrained compression flanges without mid angle and unrestrained compression flanges with mid angle.

Restraining compression flanges without mid angle is more effective than using mid angle without restraining compression flanges in case of using both straps (Table 8), within range +(0~7) % as in Fig 47. For using upper straps only and without straps the moment capacity increased within (5~20)% for lap length ranging from (0.2L to 0.5L) and from (20-30)% for lap length 0.1L. The effectiveness of using bolts is directly proportional to height of section and inversely proportional to the overlap length from (0.1L to 0.4L) in case of upper straps only (Fig 48) and from (0.1L to 0.3L) in case without straps (Fig 49). Since in case with both

straps, the failure is due to material failure so using of mid angle or bolts has no effect. But for other cases, Failure is due to geometric failure, therefore using them has an effect. And as the failure mode is distortional buckling in bottom flanges that made restraining compression flanges are more effective

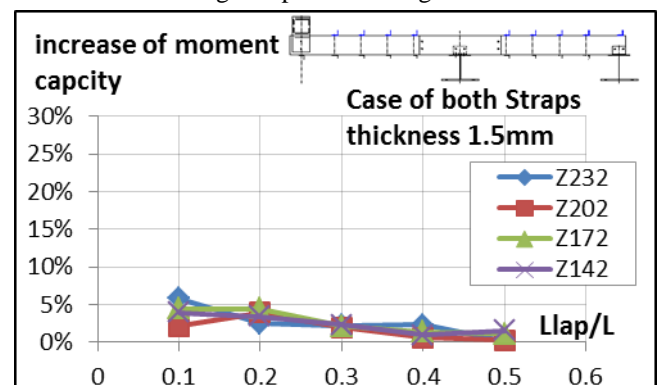


Fig 47. result of different overlaps in case of both straps

than using mid angle.

Table 8. Results of different lap lengths with both strap

Model	Lap length (mm)	Restrained compression flanges without mid angle	Unrestrained compression flanges with mid angle
		Moment capacity (m.t)	Moment capacity (m.t)
Z232	150	1.08	1.01
	300	1.35	1.31
	450	1.49	1.46
	600	1.63	1.59
	750	1.72	1.72
Z202	150	0.88	0.86
	300	1.14	1.10
	450	1.24	1.22
	600	1.34	1.34
	750	1.45	1.45
Z172	150	0.75	0.72
	300	0.96	0.92
	450	1.04	1.02
	600	1.13	1.12
	750	1.23	1.21
Z142	150	0.60	0.57
	300	0.73	0.71
	450	0.81	0.79
	600	0.88	0.87
	750	0.95	0.94

V. CONCLUSIONS

The proposed F.E. model is in good agreement with both experimental and AISI2007[14] code.

The moment Capacity is directly proportional to overlap length and height of section.

For lap length ranging from 0.2L to 0.5L, bolts in compression flanges can be added and no need for using mid angle as in case of :

i) both straps: Mid angles or restraining compression flanges slightly affect the moment capacity by less than 5%. Using any of one of them has the same effect. As bolts are more economic than angles so using bolts are recommended.

ii) upper straps only or without straps: Restraining compression flanges have a significant effect on moment capacity, where using bolts in compression flanges are more effective than using mid angles with (5-20)%.

For lap length less than 0.2L: The use of mid angles in addition to bolts in compression flanges is essential especially in heights ranging from (202mm and 232mm). As using of mid angles has a significant effect on moment capacity i)in case of upper straps only and without straps, where it increased by (25-35)% ii)in case of both straps it increased by (5-20)%.

REFERENCES

- [1] Pham, C.H. and G.J. Hancock, Numerical simulation of high strength cold-formed purlins in combined bending and shear. Journal of Constructional Steel Research, 2010. 66(10): p. 1205-1217.
- [2] Silvestre, N. and D. Camotim, Distortional buckling formulae for cold-formed steel C and Z-section members: Part I—derivation. Thin-Walled Structures, 2004. 42(11): p. 1567-1597.
- [3] Wang, H. and Y. Zhang, Experimental and numerical investigation on cold-formed steel C-section flexural members. Journal of Constructional Steel Research, 2009. 65(5): p. 1225-1235.
- [4] Yu, C. and B.W. Schafer, Distortional buckling of cold-formed steel members in bending. 2005, American Iron and Steel Institute.
- [5] Pham, C.H., A.F. Davis, and B.R. Emmett, Numerical investigation of cold-formed lapped Z purlins under combined bending and shear. Journal of Constructional Steel Research, 2014. 95: p. 116-125.
- [6] Ho, H. and K. Chung, Experimental investigation into the structural behaviour of lapped connections between cold-formed steel Z sections. Thin-Walled Structures, 2004. 42(7): p. 1013-1033.
- [7] Ghosn, A.A. and R.R. Sinno, Governing stresses in Z-purlin lap joints. Journal of Structural Engineering, 1995. 121(12): p. 1735-1741.
- [8] Ain Shams and Zamil Steel Experimental Programm.
- [9] Hancock, G.J., Cold-formed steel structures. Journal of Constructional Steel Research, 2003. 59(4): p. 473-487.
- [10] Nelson, G., H. Manbeck, and N. Meador, Cold-Formed Steel Design, in Light Agricultural and Industrial Structures. 1988, Springer. p. 283-357.
- [11] Yu, W.-W. and R.A. LaBoube, Cold-formed steel design. 2010: John Wiley & Sons.
- [12] Newman, A., Metal Building Systems-Design and specification.
- [13] ANSYS, I., ANSYS advanced analysis techniques guide. Ansys Help, 2007.
- [14] AISI 2007 -North American Specification for the Design of Cold.

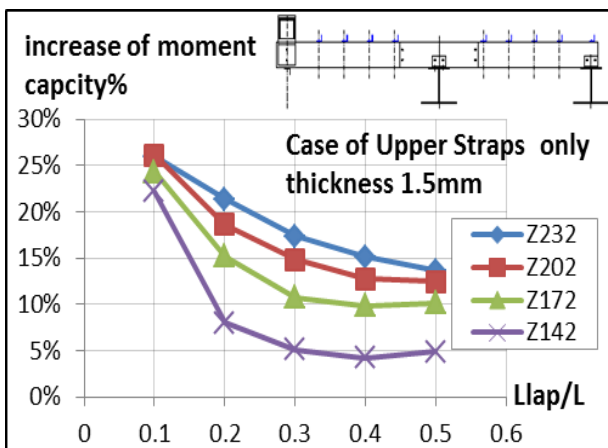


Fig 48.result of different overlaps in case of upper straps.

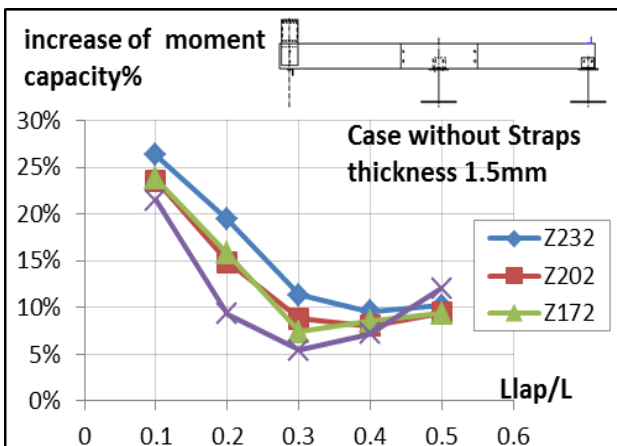


Fig 49.Result of different overlaps in case without straps.